ISSN (Print) 1226-1750
ISSN (Online) 2233-6656
Journal of Magnetics 23(2), 274-279 (2018) https://doi.org/10.4283/JMAG.2018.23.2.274

Study on Microstructure and Coercivity of Thermally Processed Nd-Fe-B–type HDDR Material

K. M. Kim[1,4], M. S. Kang[1], H. W. Kwon[1], T. H. Kim[2], C. W. Yang[3], J. G. Lee[4]*, and J. H. Yu[4]

[1]*Pukyong National University, Busan 48513, Republic of Korea*
[2]*Ames Laboratory, Ames, IA 50011, USA*
[3]*Sungkyunkwan University, Suwon 16419, Republic of Korea*
[4]*Korea Institute of Materials Science, Changwon 51508, Republic of Korea*

(Received 6 March 2018, Received in final form 12 June 2018, Accepted 12 June 2018)

Variation of intrinsic coercivity of the HDDR-treated $Nd_{12.5}Fe_{80.8}B_{6.4}Ga_{0.3}$ alloy after heating in various modes was investigated. Influence of vacuum degree and cooling after heating on the coercivity of the HDDR material was examined. The heat-treated HDDR material had consistently higher coercivity when it was quenched after heating compared to when slow-cooled. Higher coercivity in the quenched material was attributable to the grain boundary with lower Fe content. HDDR-treated material heated in high vacuum showed consistently higher coercivity than the material heated in lower vacuum, and this was attributed to less heavily oxidized surface. Reduced coercivity of the HDDR-treated material heated at moderate temperature was noticeably recovered at higher temperature, and this was attributed to lower Fe content in the grain boundary.

Keywords : Nd-Fe-B-type HDDR material, microstructure, coercivity

1. Introduction

Share of an environment-friendly vehicle (HEV, EV) in a car market has drastically ballooned these days, and permanent magnet plays a vital role in traction motor of those vehicles. Magnet used in the traction motor of the vehicles is exclusively Nd-Fe-B-type by virtue of its superior magnetic performance. However, one of the downsides of Nd-Fe-B-type magnet is its rather low Curie temperature (~315 °C), and worse still, its operating temperature in the traction motor is unavoidably high (> 150 °C). The magnet, therefore, severely lacks thermal stability, in particular a poor thermal stability of coercivity is a major problem. As such, coercivity enhancement is a hot issue in the area of Nd-Fe-B-type magnet, and common approaches for enhancing coercivity in the magnet are; (1) substitution of some Nd atoms in the $Nd_2Fe_{14}B$ phase by heavy rare earth (HRE) atoms, such as Tb or Dy [1, 2], (2) grain refinement [3, 4]. Enhancing coercivity by grain refinement is increasingly attracting great interest because it can avoid the use of expensive and scarce HRE. It would be desirable, therefore, to use a fine grain structured material like HDDR-treated Nd-Fe-B-type powder as starting material for fabrication of bulk magnet with high coercivity because the HDDR-treated Nd-Fe-B-type material inherently possesses fine $Nd_2Fe_{14}B$ grain structure. Several attempts have been made to exploit the HDDR powder as a starting material for consolidated bulk magnet with the intention of achieving high coercivity, but with little success [5-8]. As consolidation of powder material commonly requires thermal processing, insight into the influence of thermal heating on the coercivity of the Nd-Fe-B-type HDDR material can hint at finding the best way for preparing high coercivity magnet. In the present study much emphasis was placed on the link between coercivity and grain boundary feature in the thermally processed Nd-Fe-B-type HDDR material.

2. Experimental Work

$Nd_{12.5}Fe_{80.8}B_{6.4}Ga_{0.3}$ alloy was HDDR-treated in a standard condition; hydrogenation at 350 °C for 60 min under 0.1 MPa hydrogen gas, disproportionation at 820 °C for 45 min under the 0.03 MPa hydrogen pressure, desorption and recombination at 820 °C for 30 min under

*Corresponding author: Tel: +82-55-280-3606
Fax: +82-55-280-3333, e-mail: jglee36@kims.re.kr

a vacuum. The HDDR-treated powder with initial intrinsic coercivity of 14 kOe was swiftly heated up to desired temperature in controlled vacuum : high vacuum with around 5×10^{-6} mbar or lower vacuum with around 2×10^{-4} mbar. Cooling of the sample after heating was also performed in different mode quenching or slow-cooling (took approximately 30 min. from 900 ºC to 500 ºC). Description of the heating modes are shortened hereafter for convenience: HVQ and HVSC denote heating in high vacuum and then quenched or slow-cooled, and LVQ and LVSC heating in lower vacuum and then quenched or slow-cooled, respectively. Magnetic characterization of the materials was performed by VSM after magnetizing with 5 T pulsing field. Microstructure of the material was examined using scanning electron microscopy (SEM), transmission electron microscopy (TEM) and chemical analysis was performed by using energy dispersive X-ray spectroscopy (EDS).

3. Results and Discussion

Figure 1 shows variations of intrinsic coercivity of the HDDR-treated Nd-Fe-B-type material after heating in different mode. It was apparent that coercivity of the HDDR-treated material was markedly affected by the heating, and the extent of how markedly affected was dependent upon the degree of vacuum and cooling rate it had been subjected to. First and most of all, coercivity of the HDDR-treated material was markedly affected by the cooling rate: The quenched materials exhibited consistently higher coercivity with respect to the slow-cooled materials.

Although the dwelling time at higher temperature range may be slightly longer for the slow-cooled material, such a slight difference in thermal profile may cause little to none of influence on the microstructure, in particular grain structure of the materials. This was verified by microstructure observation. As shown in Fig. 2, no apparent difference in grain structure was observed in the quenched or slow-cooled materials. The average grain size in the initial, quenched and slow cooled materials were estimated to be around 0.35 um, 0.3 um and 0.36 um, respectively. This suggests that difference in the thermal profile may not be an apparent reason for the noticeably lower coercivity in the slow-cooled material compared to the quenched material. The common belief about coercivity of the Nd-Fe-B-type material is that a clear-cut link between coercivity and grain boundary characteristics exists. Grain boundaries of the quenched

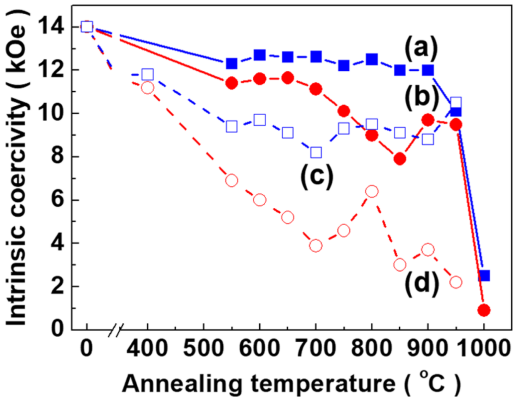

Fig. 1. (Color online) Variations of intrinsic coercivity of the HDDR-treated $Nd_{12.5}Fe_{80.8}B_{6.4}Ga_{0.3}$ alloy after heating in different mode. (a) HVQ, (b) HVSC, (c) LVQ, and (d) LVSC.

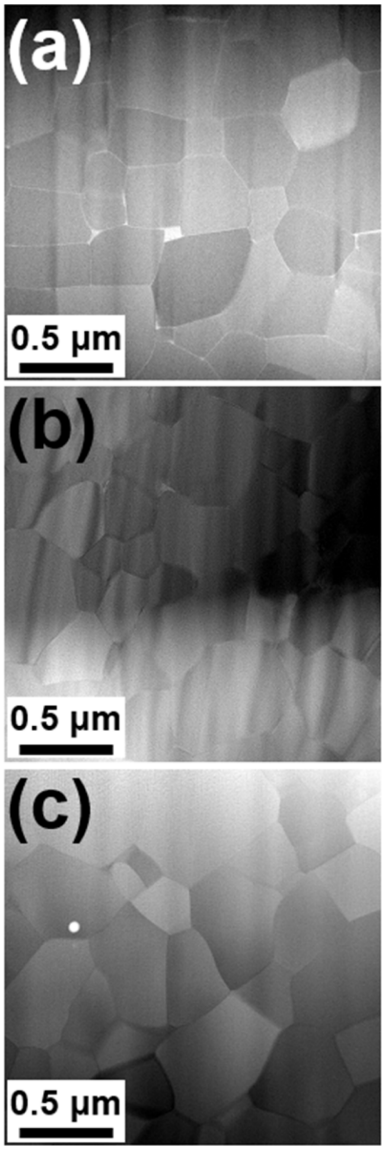

Fig. 2. Grain structure of the HDDR-treated $Nd_{12.5}Fe_{80.8}B_{6.4}Ga_{0.3}$ alloy. (a) initial, and after heating up to 850 ºC in (b) HVQ or (c) HVSC mode.

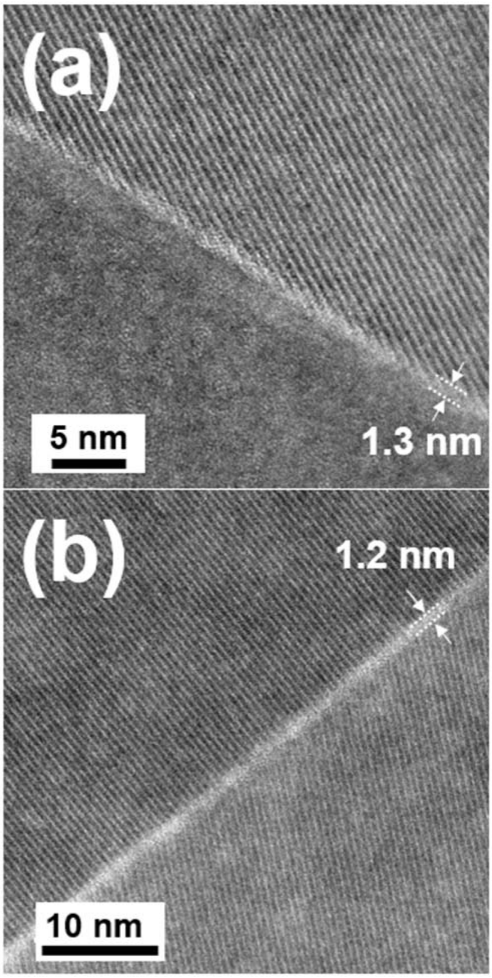

Fig. 3. TEM photos showing grain boundary structure in the HDDR-treated $Nd_{12.5}Fe_{80.8}B_{6.4}Ga_{0.3}$ alloy after heating up to 850 °C in (a) HVQ and (b) HVSC mode.

or slow-cooled materials were examined in great detail. Fig. 3 shows grain boundary in the material quenched or slow-cooled from 850 °C. In both materials, well-developed grain boundary in approximately 1.3 nm thick was observed, and no apparent difference in the grain boundary structure was found. However, what differentiates the grain boundary in the slow-cooled material from that in the quenched material was chemical composition of the grain boundaries. As summarized in Table 1, chemical composition, in particular content of the ferromagnetic element Fe in the grain boundary in the quenched or slow-cooled materials was significantly different; grain boundary in the slow-cooled material was more enriched with Fe compared to that in the quenched material. More Fe-enriched grain boundary is believed in a general sense to be more ferromagnetic. More ferromagnetic grain boundary enriched with Fe in the slow-cooled material less effectively decoupled the neighbouring grains, hence

Table 1. Chemical composition of grain boundary in the HDDR-treated $Nd_{12.5}Fe_{80.8}B_{6.4}Ga_{0.3}$ alloy in initial state and after heating up to 850 °C in HVQ and HVSC mode.

(at%)

		Nd	Fe	O	Ga
initial	G.B. 1	32.6	47.1	11.8	8.5
	G.B. 2	42.1	33.8	17.4	6.6
HVQ	G.B. 1	19.1	47.1	31.8	2.0
	G.B. 2	31.2	40.3	27.0	1.5
HVSC	G.B. 1	18.6	69.7	9.3	2.4
	G.B. 2	19.5	68.2	10.5	1.8

leading to a reduction of coercivity. The exact reason for the Fe enrichment in the grain boundary of slow-cooled material is not entirely clear, but it may be related to the solubility variation of Fe atoms in the liquid Nd-rich grain boundary phase. It is guessed that solubility of Fe in the liquid Nd-rich grain boundary phase would be limited at higher temperature. It is worth noting that grain boundary thickness in the HDDR-treated Nd-Fe-B-type material was approximately 1.3 nm, and this is seemingly not thick enough to prevent the exchange coupling between neighbouring grains. For an effective decoupling between neighbouring grains in Nd-Fe-B-type material the grain boundary thickness is needed to be at the very least comparable to the exchange length (L_{ex}) of the material, which is known to be approximately 2 nm [9]. Despite much finer grain size in the HDDR-treated Nd-Fe-B-type material with respect to other type of magnet such as sintered one, coercivity of the HDDR-treated material is usually not noticeably higher than that of sintered magnet. This may be due in large part to the insufficient grain boundary thickness in the HDDR-treated material.

Another interesting finding was that coercivity of the Nd-Fe-B-type HDDR-treated material was damaged worse when it was heated in lower vacuum, and the coercivity was even worsened in the slow-cooled material compared to the quenched one. More radical reduction of coercivity in the material heated in lower vacuum than in high vacuum may be attributable to surface oxidation. Fig. 4 shows surface microstructure of the particle heated in high or lower vacuum. The material heated in lower vacuum was heated up to 700 °C and then slow-cooled, while the material heated in high vacuum was heated up to even higher temperature of 850 °C and then slow-cooled. Although both the materials had been oxidized near surface, oxidation depth was much greater (around 1 μm) in the material heated in lower vacuum than in the material heated in high vacuum (around 0.5 μm). In addition, oxidation further proceeded along inner grain boundaries in the material heated in lower vacuum (Fig

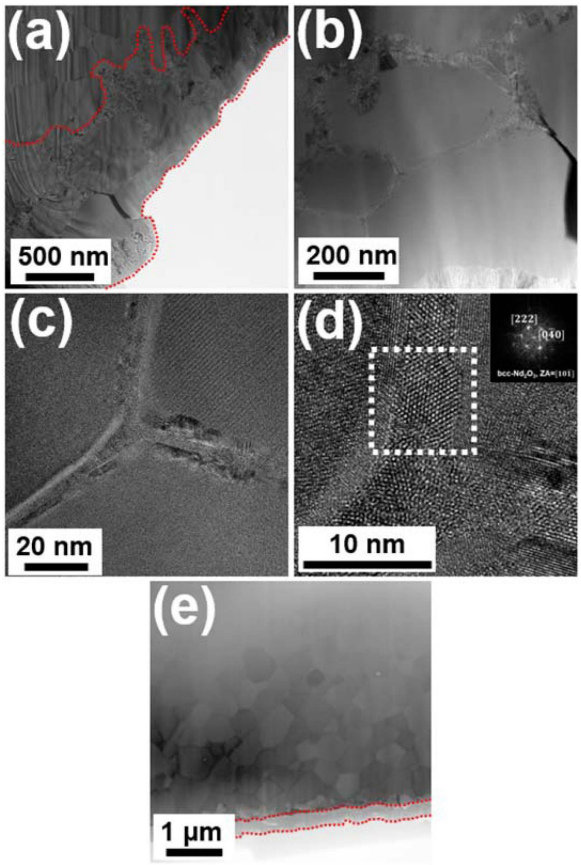

Fig. 4. (Color online) TEM photos showing surface oxidation of the HDDR-treated $Nd_{12.5}Fe_{80.8}B_{6.4}Ga_{0.3}$ alloy particle heated (a-d) up to 700 °C in LVSC and (e) up to 850 °C in HVSC mode.

4(b, c)). The oxidized grain boundary region consisted mostly of bcc-Nd_2O_3 phase (Fig. 4(d)). The oxidized region may have much lowered magnetocrystalline anisotropy, thus demagnetization may more easily initiate in this region. Therefore, the material heated in lower vacuum, which had more heavily oxidation surface, may have lower coercivity than the material heated in high vacuum. Although the volume of oxidation-damaged surface was very small in the particle (around 150 μm diameter), coercivity of the particles was radically influenced. Previous reports revealed that coercivity of the Nd-Fe-B-type fine particles was radically affected by the surface condition [6, 10-12].

It is worth remarking that demagnetization curve of the heat-treated HDDR material was also affected by heating mode. Fig. 5 shows demagnetization curves of the HDDR-treated material after heating up to 900 °C in different mode. Also included in Fig. 5 is demagnetization curve of the initial HDDR-treated material for comparison. While demagnetization curves of the materials heat treated up to

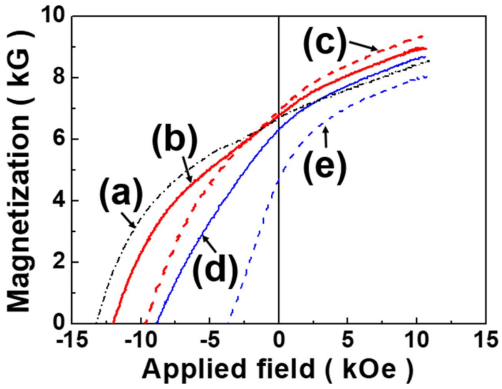

Fig. 5. (Color online) Demagnetization curves of the HDDR-treated $Nd_{12.5}Fe_{80.8}B_{6.4}Ga_{0.3}$ alloy after heating up to 900 °C in different mode. (a) initial, (b) HVQ, (c) HVSC, (d) LVQ, and (e) LVSC.

900 °C in HVSC, LVQ, or LVSC were noticeably spoilt, that of the material heat treated in HVQ remained almost intact with the exception of slight loss of coercivity and remanence. Present findings suggest that HDDR-treated material have good stability against heating if the material heated in good vacuum. The materials could hold up good demagnetization curve even after prolonged annealing at moderate temperature in good vacuum. HDDR-treated material was heated in high vacuum at 800 °C for prolonged period of as long as 360 min, and it still exhibited high coercivity and more importantly, un-spoilt demagnetization curve as shown in Fig. 6. It is noted that demagnetization curves in Fig. 6 were from aligned materials, and the alignment was done with the intention of standing out the good demagnetizing feature. Grain structure of the material annealed in high vacuum at 800 °C for prolonged period of 360 min was not radically different from that of initial material with the exception of slight grain growth as shown in Fig. 7.

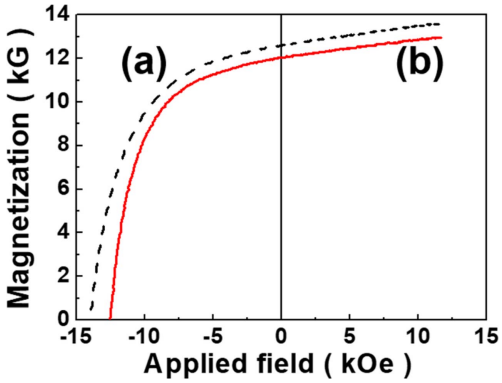

Fig. 6. (Color online) Demagnetization curves of the HDDR-treated $Nd_{12.5}Fe_{80.8}B_{6.4}Ga_{0.3}$ alloy. (a) initial, (b) after heating at 800 °C for prolonged period of 360 min in HVQ mode.

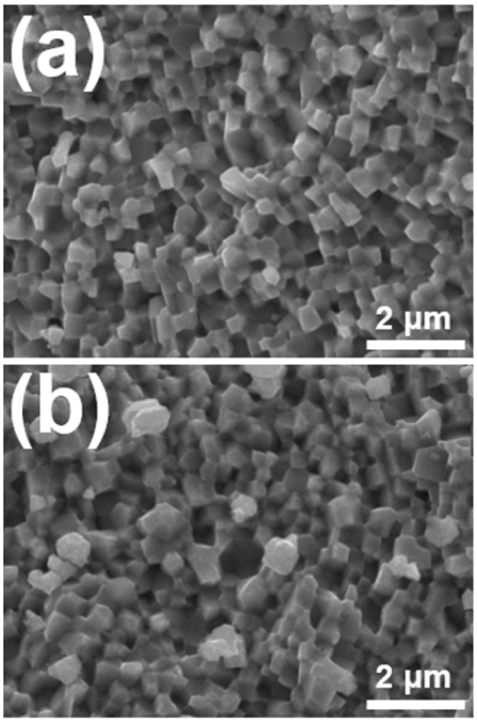

Fig. 7. SEM photos showing grain structure of the HDDR-treated $Nd_{12.5}Fe_{80.8}B_{6.4}Ga_{0.3}$ alloy. (a) initial, (b) after heating at 800 °C for prolonged period of 360 min in HVQ mode.

Finally, still wondering is that coercivity of the HDDR-treated material was reduced at moderate temperature and then markedly recovered at higher temperature. This coercivity recovery was more obvious in all samples except the material heated in HVQ mode. Fig. 8 shows grain boundary structure of the materials in reduced and recovered coercivity condition. In both the materials, grain boundary has been well developed and its thickness was also similar: approximately 1.2 nm and 1.5 nm, respectively. Grain boundary structure in both the materials was more or less similar, but chemical composition of the grain boundary in the materials was significantly different as shown in Table 2. What matters most in the chemical composition was the content of ferromagnetic element Fe. Grain boundary in the material in the reduced coercivity condition was more enriched with Fe compared to that in the material in the recovered coercivity condition. The Fe-depleted grain boundary can more effectively decouple the neighbouring grains, hence leading to recovery of coercivity.

Table 2. Chemical composition of grain boundary in the HDDR-treated $Nd_{12.5}Fe_{80.8}B_{6.4}Ga_{0.3}$ alloy in initial state after heating up to 850 °C and 900 °C in HVSC mode.

(at%)

		Nd	Fe	O	Ga
initial	G.B. 1	32.6	47.1	11.8	8.5
	G.B. 2	42.1	33.8	17.4	6.6
850 °C	G.B. 1	18.6	69.7	9.3	2.4
	G.B. 2	19.5	68.2	10.5	1.8
900 °C	G.B. 1	26.5	52.7	18.7	2.1
	G.B. 2	30.5	49.0	18.2	2.2

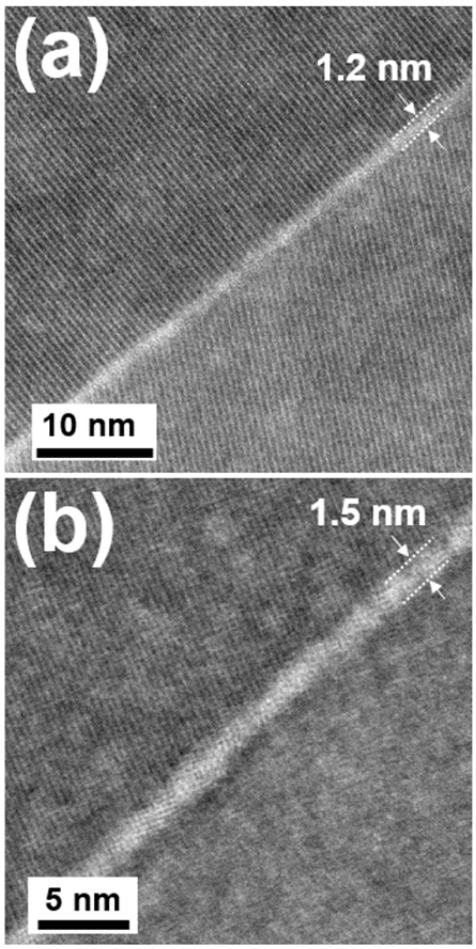

Fig. 8. TEM photos showing grain boundary structure of the HDDR-treated $Nd_{12.5}Fe_{80.8}B_{6.4}Ga_{0.3}$ alloy after heating up to (a) 850 °C and (b) 900 °C in HVSC mode.

4. Conclusion

Heat-treated $Nd_{12.5}Fe_{80.8}B_{6.4}Ga_{0.3}$ HDDR material exhibited consistently higher coercivity when it was quenched compared to when slow-cooled. Higher coercivity in the quenched material was attributable to the grain boundary with lower Fe content. HDDR-treated material heated in high vacuum showed consistently higher coercivity than the material heated in lower vacuum, and this was attributed to less heavily oxidized surface.

Reduced coercivity of the HDDR-treated material heated at moderate temperature was noticeably recovered at higher temperature, and this was attributed to lower Fe content in the grain boundary.

Acknowledgement

This work was supported by the Technology Innovation Program (10080382) funded by the Ministry of Trade, Industry & Energy (MOTIE, Korea).

References

[1] J. F. Herbst, Rev. Mod. Phys. **63**, 819 (1991).
[2] G. Yan, P. J. McGuiness, J. P. G. Farr, and I. R. Harris, J. Alloys Compd. **491**, L20 (2010).
[3] H. Sepehri-Amin, Y. Une, T. Ohkubo, K. Hono, and M. Sagawa, Scripta Mater. **65**, 396 (2011).
[4] R. Goto, S. Sugimoto, M. Matsuura, N. Tezuka, Y. Une, and M. Sagawa, Paper Presented at the 21st Workshop on Rare-Earth Permanent Magnets and Their Applications, Bled, Slovenia (2010) pp 193-196.
[5] M. Nakamura, M. Matsuura, N. Tezuka, S. Sugimoto, Y. Une, H. Kubo, and M. Sagawa, Appl. Phys. Lett. **103**, 022404 (2013).
[6] K. Takagi, M. Akada, R. Soda, and K. Ozaki, J. Magn. Magn. Mater. **393**, 461 (2015).
[7] G. Ding, S. Guo, L. Cai, L. Chen, J. Liu, D. Lee, and A. Yan, IEEE Trans. Magn. **51**, 2102304 (2015).
[8] T. Sasaki, T. Ohkubo, Y. Une, H. Kubo, and M. Sagawa, The Minerals, Metals, and Materials Society 2017 146th Annual Meeting and Exhibition, San Diego, California, USA, (2017).
[9] J. M. D. Coey, Magnetism and Magnetic Materials, Cambridge University Press (2010) p 266.
[10] Y. Li, H. E. Evans, I. R. Harris, and I. P. Jones, Oxid. Met. **59**, 167 (2003).
[11] H. W. Kwon and J. H. Yu, J. Korean Magn. Soc. **22**, 85 (2012).
[12] H. W. Kwon, J. G. Lee, and J. H. Yu, J. Appl. Phys. **115**, 17A727 (2014).